Proteomic Analysis Reveals Multiple Patterns of Response in Cells Exposed to a Toxin Mixture

Gian Luca Sala,[†,‡] Giuseppe Ronzitti,[†,‡,§] Makoto Sasaki,[||] Haruhiko Fuwa,[||] Takeshi Yasumoto,[⊥] Albertino Bigiani,[†] and Gian Paolo Rossini*[,†]

Centro Interdisciplinare di Scienze e Tecnologie per la Qualità e Sicurezza degli Alimenti, Dipartimento di Scienze Biomediche, Università di Modena e Reggio Emilia, I-41100 Modena, Italy, Graduate School of Life Sciences, Tohoku University, Sendai 981-8555, Japan, and Okinawa Science and Technology Promotion Center, Okinawa, 904-2234, Japan

Received February 4, 2009

We have used proteomic analyses to probe the responses induced by a pair of marine biotoxins, okadaic acid (OA) and gambierol (GB), added alone or in combination to a cultured cell line and carried out a preliminary investigation into the possible interactions between toxins possessing two different molecular mechanisms of action at a cellular level. When MCF-7 cells were treated with OA, we found that cellular levels of 30 proteins were significantly affected, including several isoforms of nonphosphorylated and phosphorylated hsp 27, as well as enzymes involved in the maintenance of nucleoside triphosphate pools and the control of redox states of the cell. When we repeated our analysis using GB, nine proteins were significantly affected, including some isoforms of nonphosphorylated hsp 27, as well as semenogelin-1, myosin-7, and the ATP synthase subunit δ. The combined addition of OA and GB to MCF-7 cells, in turn, affected 14 proteins, including some isoforms of nonphosphorylated and phosphorylated hsp 27, as well as myosin-7, the ATP synthase subunit δ, and enzymes involved in the control of redox states of the cell. If components affected by either OA or GB, as well as by the combined treatment, were classified according to the detected changes, two sets of data were obtained, including the components whose levels were found affected by the combined treatment, regardless of the effect observed after addition of only one agent, and those that had been found affected in cells that had been challenged with only one toxin but not when cells had been subjected to the combined treatment. Multiple patterns of responses to the toxin mixture were recorded in the two sets, consisting of both independent and interacting actions, among which we detected synergistic, similar, and antagonistic effects.

Introduction

The use of biomarkers for the assessment of the exposure of biological entities to potential hazards, including toxic substances, is an established practice that has gained new impetus by the introduction of high-throughput technologies, with their potential to process large amounts of analytes at the same time (*1, 2*). These systemic analyses provide the fingerprints of exposures to individual groups of chemicals, avoiding the risk inherent in the use of single end point bioassays (*1*−*3*).

In the real world, living organisms are exposed to complex mixtures of bioactive compounds and hazardous chemicals, so that the identification of biomarkers for a single class of compounds may not be sufficient for a proper understanding of any molecular fingerprint. Furthermore, the possibility that mixtures of toxins at concentrations below their nonobservable adverse effect levels might cause detectable responses in biological systems should be considered (*4*).

To approach this level of complexity and taking into account the limited information regarding possible interactions between different classes of marine biotoxins in biological systems, we set out a preliminary investigation to probe the general behavior of an experimental model challenged with two different toxins. The aim of our study was to carry out a system-level analysis, to ascertain whether general patterns of responses could be found, independently of specific sequences of events set in motion by the agents present in a mixture. In this study, therefore, the biological system was treated as a black box, and we have analyzed the overall outputs generated by the chemicals added to the system (*5*).

Some methodological choices were made to develop our study. To simplify the analysis and obtain sets of data that could represent the overall responses of the system to the tested compounds at the effector level, we characterized the changes induced by biotoxins in the proteome of a cultured cell line. The use of marine biotoxins was made because contamination of seafood by algal toxins is a widespread phenomenon, posing significant threats to human and animal health (*6*), and it has long been recognized that contamination can involve multiple chemical classes of compounds (*7*−*9*), often present in contaminated materials at the same time (*9*−*12*). A second choice regarded the tested compounds, and we sought to minimize the occurrence of interactions among different biotoxins. To this end, we have challenged the experimental system with okadaic acid (OA) and gambierol (GB), because they have distinct mechanisms of action. OA, in fact, is an inhibitor of serine/threonine phosphoprotein phosphatases (*13*), whereas GB affects

* To whom correspondence should be addressed. E-mail: gianpaolo.rossini@unimore.it.
[†] Università di Modena e Reggio Emilia.
[‡] These authors have equally contributed to this paper.
[§] Present address: Neuroscience and Brain Technologies Department, Italian Institute of Technology, Via Morego 30, 16163, Genova, Italy.
[||] Tohoku University.
[⊥] Okinawa Science and Technology Promotion Center.

10.1021/tx900044p CCC: $40.75
Published on Web 04/27/2009

potassium channels (*14*). In this paper, we report that cells exposed to a mixture of marine biotoxins acting through distinct molecular mechanisms display multiple patterns of response at a proteome level.

Experimental Procedures

Materials. OA was purchased from Alexis Biochemicals. GB was synthesized as already described (*15*). Toxins were diluted in absolute ethanol and stored at −20 °C.

All chemicals used to carry out two-dimensional (2D) electrophoresis were from Bio-Rad. All other chemicals were from Sigma.

Cell Culture Conditions and Toxin Treatments. MCF-7 cells were obtained from the European Collection of Animal Cell Cultures (ECACC No. 86012803 CB No. 2705) and were grown in 5% carbon dioxide in air at 37 °C, in 90 mm diameter Petri dishes, with a culture medium composed of Dulbecco's modified Eagle's medium, containing 1% nonessential amino acids and 10% fetal calf serum, as previously described (*16*).

Cells in logarithmic growth received either 50 nM OA, 50 nM GB, or both toxins at a final concentration of 50 nM. Control cells received an equal volume of absolute ethanol. After 24 h of incubation at 37 °C, cells were harvested and processed to obtain extracts.

Preparation of Cell Extracts. All of the steps were performed at 4 °C. The culture medium from every Petri dish was collected and centrifuged for 10 min at 800*g*. Cells from every dish were washed with 5 mL of 20 mM phosphate, pH 7.4, and 0.15 M NaCl (PBS buffer). Cells were then mechanically detached from culture plates with a scraper. The cell suspension was combined with the cell pellet obtained from its culture medium, and the sample was then centrifuged for 10 min at 800*g*. The cell pellet was washed twice by resuspension in 5 mL of PBS and centrifugation for 10 min at 800*g*.

Cells were then lysed by resuspension in 8 M urea, 2% CHAPS, 0.2% Biolyte Ampholyte, 50 mM DTT, 0.1 mg/mL PMSF, and 1 mM Na_3VO_4 (0.16 mL/dish), followed by vortexing of the cell suspension, and the lysate was next centrifuged for 60 min at 110000*g*. The supernatant of this centrifugation was saved, its protein content was determined according to Bradford (*17*), and the extract was then used for protein separation by 2D electrophoresis.

Two-Dimensional Electrophoresis. Protein separation by 2D electrophoresis was carried out according to Bjellqvist et al. (*18*). Samples containing the same total amount of protein were first subjected to isoelectrofocusing on polyacrylamide gels immobilized on inert support, with a nonlinear pH gradient between 3 and 10 (Bio Rad, Readystrip IPG pH 3−10 nonlinear 17 cm). The run protocol consisted of 4 h of passive rehydration, followed by 8 h of active rehydration at 50 V, 30 min at 250 V, 10000 V until 60000 V/h, and then 500 V until the end of the run.

At the end of focusing, the IPG strips were reduced by treatment with 6 M urea, 0.375 M Tris, pH 8.8, at 25 °C, 2% SDS, 20% glycerol, and 2% w/v DTT for 15 min. The material was next subjected to the alkylation reaction by treatment with 6 M urea, 0.375 M Tris, pH 8.8, at 25 °C, 2% SDS, 20% glycerol, 0.01% bromo phenol blue, and 2.5% w/v iodoacetamide for 15 min.

After reduction and alkylation, the strips were orthogonally loaded onto 12.5% acrylamide/bisacrylamide (37.5:1) gels, containing 0.1% SDS in 0.375 M Tris, pH 8.8, at 25 °C. The electrophoresis was next performed at 200 constant V. At the end of the electrophoresis, the proteins in the gels were detected by silver stain (*19*). Spots were excised from the gels and were subjected to tryptic digestion (*20*), before being analyzed by electrospray ionization mass spectrometry (ESI-MS), using Micromass Q-TOF.

Digital Elaboration and Statistical Analysis of Experimental Data. To reduce the effect of sample variability, results were derived from at least three distinct experiments, in which each cell extract was analyzed by at least two gels, run in parallel, and used for the digital analysis. The colored gels were converted into digital images by GS-800 (Bio-Rad) scanner acquisition. The files so acquired were processed with the software PDQuest (Bio-Rad), to obtain a virtual gel from the superimposition of all of the single gels subjected to analysis. The protein profiles from treated samples were then matched with those of controls, to identify qualitative and quantitative differences. The significance of experimental data was set by the software, with a cutoff value of 1 ± 0.2 for the detection of *n*-fold differences. Within the data sets yielded by the software, outliers were identified by the Grubbs test ($\alpha = 0.05$), and detected changes were retained for further analysis when they reached a significance at the 95th percentile by the Student's *t* test.

Results

Effect of Individual Toxins on the Protein Profiles of MCF-7 Cells. The biological system of this study was chosen based on available knowledge on the toxicity of OA and GB. In vivo, the major cellular targets of OA are epithelia (*21*), whereas those of GB remain uncertain, although the action exerted by this toxin on voltage-gated potassium channels (VGKCs) (*14*) indicate that they could consist of excitable cells. To limit the expected differences between the target cells of the two toxins, we chose MCF-7 cells as an experimental model, because they have been shown to be a target of OA (*16, 22, 23*) and express several isoforms of VGKCs (*24*). The experimental conditions that we chose included OA and GB concentrations that we found to induce optimal responses in our experimental systems (*14, 16*). Furthermore, the duration of toxin treatments was set to 1 day, to maximize the detection of changes in the cell proteome, taking into account that protein turnover occurs in time frames of hours to days (*25*) and limiting the cytotoxic effects of OA detectable after prolonged exposure of MCF-7 cells (*16, 26, 27*).

Initial experiments were carried out to characterize the changes in the protein profile of MCF-7 cells caused by each of the toxins used in this study. Cell cultures were then treated for 1 day with 50 nM OA, and the cell extracts were prepared from OA-treated and control cells. The separation of proteins in the extracts by 2D gel electrophoresis (Figures S1 and S2 of the Supporting Information) yielded profiles containing several hundreds of different components. The statistical analysis of the results obtained in three separate experiments revealed 30 components whose levels were significantly ($p < 0.05$) affected by OA treatment in a qualitative/quantitative fashion. Figure 1 summarizes these data and shows that most of the changes that we detected included a quantitative increase, or decrease, in the levels of a protein already expressed in the cell, such as components SSP 4101 and SSP 7307 (Figure 1), but we also observed that OA treatment caused the induction or the repression of cellular proteins, as in the case of components SSP 2109 and SSP 5006 (Figure 1).

We next repeated our experiments using GB and compared the protein profiles of extracts prepared from control and GB-treated MCF-7 cells. The separation of proteins in the extracts by 2D gel electrophoresis (Figure S3 of the Supporting Information) and the statistical analysis of the results obtained in three separate experiments revealed only nine components whose levels were significantly ($p < 0.05$) changed by GB treatment, leading to either an increase or a decrease of their cell levels, as in the case of SSP 5409 and SSP 7110, respectively (Figure 2). Six of those components had been found affected also by OA treatment (Figures 1 and 2).

Combined Effect of OA and GB on the Protein Profile of MCF-7 Cells. The characterization of major changes induced in the protein profile of MCF-7 cells by OA and GB, individually added to culture medium, allowed us to proceed with the analysis of alterations induced by exposing cells to a mixture of the two toxins. The combined addition

	Control			+ Okadaic Acid					
SSP	Mean	±	SD	Mean	±	SD	t	nfold	p
7307	1950.62	±	241.15	818.88	±	167.58	8.86	0.42	0.001
4101	166.68	±	129.76	1785.40	±	489.70	7.78	10.71	
3006	438.20	±	170.68	1337.62	±	287.11	6.43	3.05	
3010	2141.63	±	271.20	647.75	±	591.76	5.53	0.30	0.01
2109	3.46	±	2.88	2590.42	±	1194.02	5.31	748.68	
8013	2311.34	±	870.35	398.47	±	179.83	4.83	0.17	
2008	1019.26	±	291.01	341.88	±	187.18	4.49	0.34	
9901	481.94	±	202.41	60.62	±	82.26	4.36	0.13	
3106	3.46	±	2.88	5015.50	±	2816.24	4.36	1449.57	
6101	747.12	±	196.72	354.95	±	51.02	4.34	0.48	
7305	980.12	±	289.76	388.83	±	130.46	4.22	0.40	
5003	2616.46	±	645.52	1252.82	±	403.55	4.10	0.48	
6105	1133.48	±	386.11	448.88	±	35.76	3.95	0.40	
8503	675.28	±	248.10	146.48	±	193.02	3.89	0.22	
8012	2396.34	±	777.59	1052.30	±	159.97	3.80	0.44	
9301	9368.82	±	1839.19	4422.18	±	2495.59	3.78	0.47	
2106	1498.82	±	445.81	700.68	±	177.16	3.76	0.47	
8005	1749.32	±	667.95	3066.70	±	460.92	3.73	1.75	0.05
5113	1178.86	±	368.23	445.37	±	281.20	3.65	0.38	
2005	7563.78	±	3299.30	2090.18	±	650.15	3.65	0.28	
9101	312.06	±	167.67	35.22	±	32.77	3.63	0.11	
5004	560.68	±	157.20	182.22	±	205.95	3.45	0.32	
8116	1229.18	±	476.09	482.18	±	96.55	3.45	0.39	
6004	1075.80	±	357.20	368.53	±	321.99	3.42	0.34	
4109	29.05	±	15.82	447.83	±	300.39	3.41	15.42	
7001	722.36	±	344.46	211.62	±	28.37	3.31	0.29	
202	536.92	±	23.48	266.50	±	199.29	3.30	0.50	
5010	819.26	±	554.61	7.54	±	9.12	3.27	0.01	
8003	1221.84	±	576.30	466.22	±	43.05	2.93	0.38	
5006	1019.14	±	783.83	15.40	±	16.34	2.86	0.02	

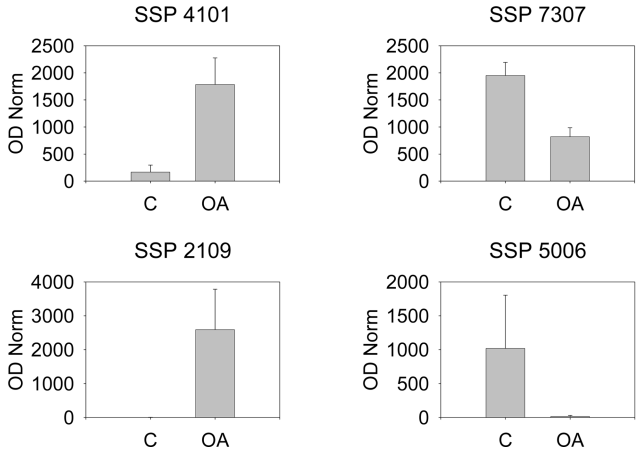

Figure 1. Effect of OA treatment of MCF-7 cells on the protein profile of total cell lysates. MCF-7 cells were treated with 50 nM OA for 24 h before being used for the preparation of cell lysates. Top: list of components (SSP) whose levels have been affected by OA treatment, as determined by the absorbances measured for indicated spots, that have been expressed as means ± SDs of values obtained from three separate experiments in triplicate. Bottom: graphical representation of the four types of changes detected in the cellular levels of components affected by OA.

of OA and GB to MCF-7 cells induced a change in their protein profile (Figure S4 of the Supporting Information), and the statistical analysis of our data revealed that the cellular levels of 14 such components were significantly ($p < 0.05$) affected (Figure 3). The changes that we detected included the quantitative increase, or decrease, in the levels of a protein already expressed in the cell, such as components SSP 4101 and SSP 7105 (Figure 3), as well as the induction, or the repression, of cellular proteins, as in the case of components SSP 3106 and SSP 5006 (Figure 3).

If the data that we obtained with the mixture of OA and GB are compared to those found when cultured cells had been challenged with the two toxins added individually, the identities and the number of components whose levels were significantly affected

	Control			+ Gambierol					
SSP	Mean	±	SD	Mean	±	SD	t	nfold	p
3010	2141.63	±	271.20	5859.51	±	1468.79	6.54	2.74	
4109	29.05	±	15.82	239.44	±	96.78	5.65	8.24	
5409	180.08	±	87.23	864.06	±	309.29	5.55	4.80	0.01
5004	560.68	±	157.20	2485.53	±	1042.57	4.81	4.43	
5113	1178.86	±	368.23	2239.14	±	396.08	4.76	1.90	
3006	438.20	±	170.68	1239.04	±	441.36	4.37	2.83	
7105	487.40	±	54.08	308.00	±	113.32	3.65	0.63	
5010	819.26	±	554.61	2102.43	±	803.19	3.27	2.57	0.05
7110	465.12	±	195.73	191.44	±	80.13	2.95	0.41	

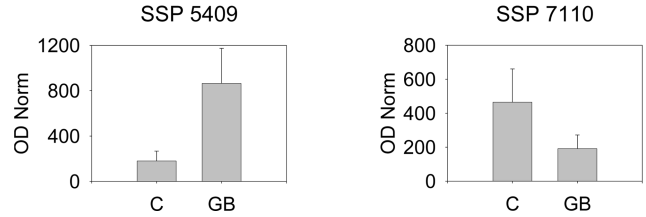

Figure 2. Effect of GB treatment of MCF-7 cells on the protein profile of total cell lysates. MCF-7 cells were treated with 50 nM GB for 24 h before being used for the preparation of cell lysates. Top: list of components (SSP) whose levels have been affected by GB treatment, as determined by the absorbances measured for indicated spots, that have been expressed as means ± SDs of values obtained from three separate experiments in triplicate. Bottom: graphical representation of the two types of changes detected in the cellular levels of components affected by GB.

by the combined treatment did not coincide with those that had been found modified after challenging of cells with only one toxin. In particular, of the 35 components found affected by either OA or GB (or both, when added separately), 12 were also significantly changed by cell treatment with the toxin mixture. In turn, two other components were found to be affected after the combined treatment and not after exposing the cells to only one toxin (Figures 1−3).

Identification of Protein Components Affected by OA and GB Treatment in MCF-7 Cells. The protein components whose levels were affected by OA and GB, either alone or in combination, were then identified by tryptic digestion of protein spots in the gels and ESI-MS of resulting peptides (Table 1). After identification, the components were analyzed using the DAVID functional annotation chart and were classified accordingly (Table S1 of the Supporting Information).

The components of the proteome affected by OA in MCF-7 cells included primarily enzymes and proteins endowed with binding activity. Several isoforms of hsp27 (β-1 protein) were identified as the components maximally affected by the toxin treatment. The peptides identified by MASCOT analysis are part of the hsp27 protein and included both phosphorylated and nonphosphorylated residues that led to the distinction of seven different isoforms (Figure 4). These proteins were identified, according to MASCOT analysis, as the intact nonphosphorylated hsp27 (SSP 5113), four phosphorylated forms, including two intact proteins that can be distinguished according to the phosphorylated serine/threonine residues (SSP 2109 and SSP 3106), and two proteolytic fragments of hsp27 (SSP 3010 and SSP 4101). The remaining two components were identified as fragments of nonphosphorylated hsp27 (SSP 4109 and SSP 5010). Of these seven proteins, the two intact phosphorylated hsp27s (SSP 2109 and 3106) represented the major forms detected in OA-treated cells. The cellular levels of the intact phosphorylated hsp27s were maximally (about 3 orders of magnitude) increased by the toxin, and this response was accompanied by a net decrease in the levels of the intact nonphosphorylated form (Table 1). The levels of the proteolytic fragments of hsp27 detected under our experimental conditions,

	Control			+ OA + GB					
SSP	Mean	±	SD	Mean	±	SD	t	nfold	p
2109	3.46	±	2.88	1947.73	±	255.15	22.86	562.93	
7105	487.40	±	54.08	170.31	±	71.10	9.36	0.35	0.001
4109	29.05	±	15.82	1576.79	±	539.17	8.61	54.28	
8002	236.16	±	118.63	936.38	±	223.18	7.66	3.97	
5409	180.08	±	87.23	775.82	±	231.02	6.90	4.31	
4101	166.68	±	129.76	1138.03	±	405.04	6.61	6.83	0.01
3106	3.46	±	2.88	4093.41	±	1940.17	6.32	1183.07	
3006	438.20	±	170.68	1027.19	±	273.26	4.96	2.34	
6106	2287.80	±	913.30	801.85	±	275.42	3.55	0.35	
8003	1221.84	±	576.30	301.59	±	233.83	3.42	0.25	
7307	1950.62	±	241.15	1502.34	±	238.63	3.35	0.77	
2106	1498.82	±	445.81	773.84	±	276.23	3.30	0.52	0.05
2008	1019.26	±	291.01	579.58	±	138.41	3.18	0.57	
5006	1019.14	±	783.83	26.86	±	20.37	2.83	0.03	

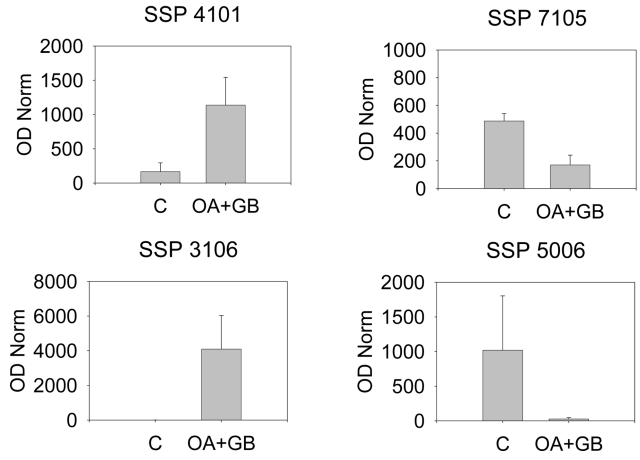

Figure 3. Effect of the combined treatment of MCF-7 cells with OA and GB on the protein profile of total cell lysates. MCF-7 cells were treated with 50 nM OA and 50 nM GB for 24 h before being used for the preparation of cell lysates. Top: list of components (SSP) whose levels have been affected by the combined treatment of MCF-7 cell with OA and GB for 24 h, as determined by the absorbances measured for indicated spots, that have been expressed as means ± SDs of values obtained from three separate experiments in triplicate. Bottom: graphical representation of the four types of changes detected in the cellular levels of components affected by the combined treatment with OA and GB.

in turn, varied depending on the individual component in OA-treated cells.

Most of the remaining proteins, whose levels were affected by OA treatment in MCF-7 cells, comprised enzymes involved in several metabolic functions, including the maintenance of nucleoside triphosphate pools (ATP synthase and nucleoside diphosphate kinase A) and the control of the redox state of the cell (for instance, superoxide dismutase 1, peroxiredoxin 5, and thioredoxin). All but one of those enzymes were found to be decreased in MCF-7 cells after OA treatment, the only exception being represented by the ATP synthase subunit δ (Table 1).

The treatment of MCF-7 cells with GB was found to affect hsp27, but the pattern of response was mostly opposed to that found after cell treatment with OA, as GB induced a limited increase in the levels of intact nonphosphorylated hsp27 and of three proteolytic fragments of hsp27 (SSP 3010, SSP 5010, and SSP 4109) (Table 1). The three remaining proteins whose levels were found increased by GB included the precursor of semenogelin-1, a major secretory protein of seminal vescicles (*28*), myosin-7, and the ATP synthase subunit δ. The combined effect of OA and GB in MCF-7 cells, in turn, led to changes in the levels of several isoforms of hsp27, of enzymes involved in the maintenance of nucleoside triphosphate pools, and the control of redox states of the cell, as well as myosin-7 (Table 1).

Patterns of Responses Induced in MCF-7 Cells by OA and GB in Combination. The identification of proteins affected by OA and GB, either alone or in combination, led to recognition that some components were shared by the responses to both toxins, whereas some of them appeared toxin-specific. To further analyze the results that we obtained, the proteins affected by those toxin treatments were divided into two sets (Tables S2 and S3 of the Supporting Information). The first set (set 1) includes the components whose levels were found to be significantly affected ($p < 0.05$) by the combined treatment, regardless of the effect observed after the addition of only one agent, whereas the second set (set 2) comprises the components that were found to be significantly affected ($p < 0.05$) in cells that had been challenged with only one toxin (either OA or GB) but not when cells were subjected to the combined treatment. The data of set 2 were next analyzed by Student's *t* tests by matching the values obtained from cells after the combined treatment to those obtained with control cells and cells that were treated with only one toxin (Table S3 of the Supporting Information). When we set the lowest limit of confidence for those changes at the 95th percentile, the 35 components of the two sets could be distributed into a matrix, comprising the full range of possible combinations (Table 2).

The graphical representations of relevant patterns of responses for the components of set 1 and set 2 are reported in Figures 5 and 6, respectively, and the results that we obtained with the remaining components of the two sets are reported in Figure S4 of the Supporting Information.

The patterns of responses that we found with the components of set 1 can be essentially reduced to three major types, each of which is grouped in the secondary sets. When results were significant in the three matchings (secondary set A) at the highest percentile ($p < 0.01$), the components of the mixture appeared to act synergistically, as in the case of SSP 8002 (or SSP 4109), and the measured effects were more than expected by the simple addition of those found with individual toxins (Figure 5A).

If the significance was found by matching with controls and only one of the treatments with a single toxin (secondary sets B and C), as in the case of SSP 5409 and SSP 2109, the effect induced by GB and OA, respectively, was maintained in the presence of the other toxin (Figure 5B,C), and the patterns of response indicated that each toxin acted independently of the other one, yielding effects that were toxin-specific.

When a significant finding was found by matching the results obtained with the mixture of toxins and the controls but was not apparent by matching the combined effect with that obtained with either of the two toxins added alone (secondary set D), the patterns of responses showed the existence of a clear effect, in terms of either increased (such as SSP 3006, Figure 5D) or decreased levels (such as SSP 8003, Figure S5 of the Supporting Information) of individual components, which was induced by either toxin added alone but was not further enhanced by treating the cells with the combination of the two toxins. In these latter cases, responses induced by a single toxin appeared to reach their maxima, and increases or decreases in the levels of components could not be further enhanced by the presence of the other toxin when administered in combination. These molecular effects were then induced by both toxins, independently, showing similar responses. Figure 6 summarizes the findings obtained with set 2, whose patterns essentially consist of antagonistic responses, in which one toxin abolished the effect induced by the other toxin, when added in combination.

Table 1. Identification of Protein Components Found in Lysates from MCF-7 Cells That Had Been Exposed to OA, GB, and the Combination of the Two Toxins[a]

SSP	seq. cov.	protein	*n*-fold	*p*
		OA		
3106	40	heat shock protein β-1	1449.57	0.050
2109	25	heat shock protein β-1	748.68	0.010
4109	4	heat shock protein β-1	15.42	0.050
4101	25	heat shock protein β-1	10.71	0.010
3006	50	ATP synthase subunit δ,	3.05	0.010
8005	58	cofilin-1	1.75	0.050
202	16	methylosome subunit pICln	0.50	0.050
5003	24	superoxide dismutase [Cu−Zn]	0.48	0.050
6101	19	protein-L-isoaspartate(D-aspartate) O-methyltransferase	0.48	0.050
9301	29	fructose-bisphosphate aldolase A	0.47	0.050
2106	29	catechol O-methyltransferase	0.47	0.050
8012	66	peptidyl-prolyl *cis*−*trans* isomerase A	0.44	0.050
7307	19	poly(rC)-binding protein 1	0.42	0.001
7305	22	sialic acid synthase	0.40	0.050
6105	11	heat shock protein β-1	0.40	0.050
8116	25	calcyclin-binding protein	0.39	0.050
8003	40	peroxiredoxin-5, mitochondrial [precursor]	0.38	0.050
5113	44	heat shock protein β-1	0.38	0.050
6004	46	mesoderm development candidate 2	0.34	0.050
2008	27	lactoylglutathione lyase	0.34	0.050
5004	49	semenogelin-1 [precursor]	0.32	0.050
3010	27	heat shock protein β-1	0.30	0.010
7001	21	40S ribosomal protein S12	0.29	0.050
2005	32	thioredoxin	0.28	0.050
8503	32	ATP synthase subunit α, mitochondrial [precursor]	0.22	0.050
8013	26	destrin	0.17	0.010
9901	19	probable ATP-dependent RNA helicase DDX17	0.13	0.050
9101	16	coiled−coil−helix−coiled−coil−helix domain-containing protein 3, mitochondrial [precursor]	0.11	0.050
5006	59	nucleoside diphosphate kinase A	0.02	0.050
5010	28	heat shock protein β-1	0.01	0.050
		GB		
4109	4	heat shock protein β-1	8.24	0.010
5004	49	semenogelin-1 [precursor]	4.43	0.010
5409	7	myosin-7	4.80	0.010
3006	50	ATP synthase subunit δ,	2.83	0.050
3010	27	heat shock protein β-1	2.74	0.010
5010	28	heat shock protein β-1	2.57	0.050
5113	44	heat shock protein β-1	1.90	0.010
7105	26	phosphoglycerate mutase 1	0.63	0.050
7110	22	fumarylacetoacetate hydrolase domain-containing protein 1	0.41	0.050
		OA + GB		
3106	40	heat shock protein β-1	1183.07	0.010
2109	25	heat shock protein β-1	562.93	0.001
4109	4	heat shock protein β-1	54.28	0.001
4101	25	heat shock protein β-1	6.83	0.010
5409	7	myosin-7	4.31	0.010
8002	16	superoxide dismutase [Mn], mitochondrial [precursor]	3.97	0.010
3006	50	ATP synthase subunit δ,	2.34	0.010
7307	19	poly(rC)-binding protein 1	0.77	0.050
2008	27	lactoylglutathione lyase	0.57	0.050
2106	29	catechol O-methyltransferase	0.52	0.050
6106	52	peroxiredoxin-6	0.35	0.050
7105	26	phosphoglycerate mutase 1	0.35	0.001
8003	40	peroxiredoxin-5, mitochondrial [precursor]	0.25	0.050
5006	59	nucleoside diphosphate kinase A	0.03	0.050

[a] The spots excised from the gels were digested with trypsin and analyzed by ESI-MS, as indicated in the Experimental Procedures. The pkl files obtained from the instruments were used in MASCOT to identify proteins. The protein list was subdivided into three tables corresponding to the OA, GB, and OA + GB treatments. In each table, the proteins are ordered based on the *n*-fold change in their level with regard to controls, and data refer only to the proteins whose levels have been significantly ($p < 0.05$) affected by the indicated treatments.

Discussion

We have approached the study of the patterns of responses of biological systems to the combined exposure to multiple toxins by a simplification of the experimental settings and have exposed the cells to agents possessing distinct mechanisms of action.

The components analyzed in the extracts that we prepared from MCF-7 cells account for a portion of the total proteome of this cell line. Still, the responses that we detected within this subset of the MCF-7 cell proteome showed distinct features, depending on the exposure to individual toxins.

The effects induced by OA were in line with its established mechanism of action, whereby the inhibition of serine/threonine phosphoprotein phosphatases (PPases) involved in the control of cellular processes (*13*) leads to the collapse of regulatory

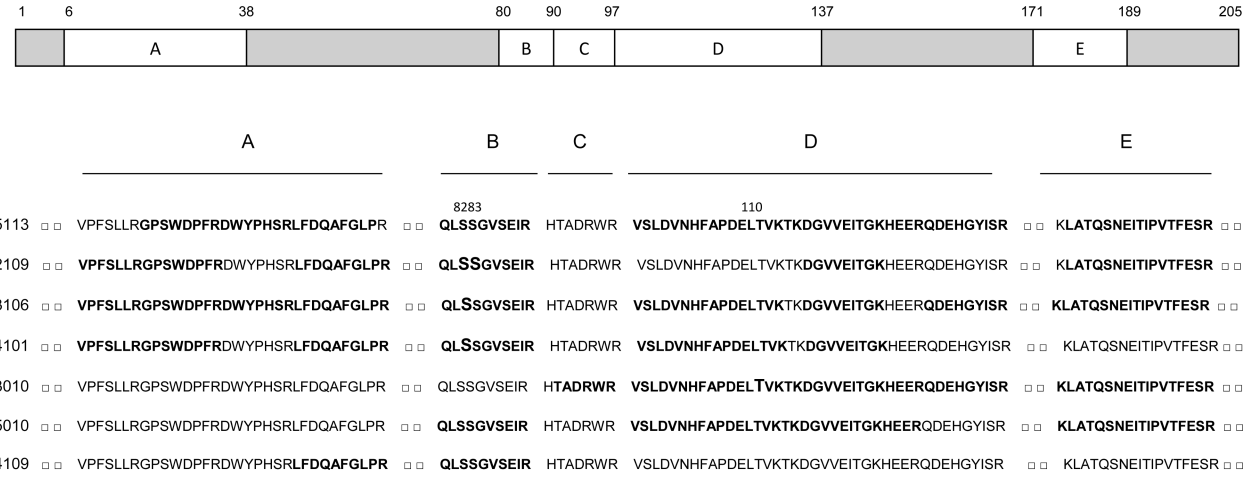

Figure 4. Characterization of major hsp27 isoforms found in MCF-7 cells exposed to OA. The experimental conditions are as reported in the legend to Figure 1 and Table 1. Schematic representation of the hsp27 molecule: The positions of the five peptides analyzed by ESI-MS in the protein sequence are indicated. Amino acid sequences of the five peptides in the seven hsp27 isoforms identified by ESI-MS. The MASCOT-recognized peptides are indicated in black, whereas the nonrecognized peptides are in gray. The amino acids phosphorylated in the peptides, as identified by MASCOT, are reported in bold letters, and the number at the top of the panel indicates the position of the amino acid in the sequence of hsp27.

mechanisms and results in cell death (*27*). The major effects that we detected in OA-treated cells, that is, the high proportion of phosphorylated forms of hsp27, as opposed to the nonphosphorylated protein, and the increase in protein fragments of hsp27, are in line with the proposed model of OA-induced cell death (*27*). The proteins of the hsp family, in fact, have a role in the protection of cells from noxious stimuli and adverse conditions, and hsp27, in particular, is known to protect cells from death (reviewed in ref *29*). This protective role is played by large, multisubunit, oligomers of hsp27 (*30*). The equilibrium between the association and the dissociation of hsp27 subunits is governed by hsp27 phosphorylation, and the phosphorylation of hsp27 favors dissociation of oligomers and the loss of protective activity of hsp27 (*31, 32*). Indeed, cell treatment with OA is known to favor the phosphorylation of hsp27 and the dissociation of oligomers (*31*), as well as the loss of protective activity against cellular stress (*32, 33*). In keeping with those observations, OA was found to increase the cellular content of the intact hsp27 phosphorylated in Ser_{82} (SSP 2109 and 3106; Figure 4 and Table 1), that is a residue phosphorylated in vivo, and is involved in down-regulation of the protective function of hsp27 (*32*).

Overall, the effects of OA most likely represent an ongoing process of cell disposal, as net decreases in the cellular content of almost all of the remaining proteins were detected (Table 1). The 3-fold increase of the ATP synthase subunit δ is the only exception that we detected (Table 1), but the contradictory nature of this finding is only apparent because increases in the cellular content of ATP synthase subunit δ have been found to accompany stress responses and cell death in other model systems (*34, 35*).

The response induced by GB in MCF-7 cells was marked by increases in nonphosphorylated hsp27 (SSP 4109, 5010, and 5113) and by an hsp27 isoform phosphorylated in $threonine_{110}$ (SSP 3910), which is not known to affect the oligomeric state and functioning of hsp27. Taking into consideration the protective role played by nonphosphorylated hsp27 in the stress response of cells to noxious stimuli (*31, 32*), the molecular features of hsp27 in MCF-7 cells exposed to GB indicate that impairment of VGKC by this toxin could cause a stress condition in MCF-7 cells, triggering a protective response. The increase in cellular ATP synthase subunit δ that we detected in cells exposed to GB (Table 1) would be in line with this interpretation. Cell death was not detected in our cultures exposed to GB alone, however, indicating that the adaptive mechanisms of cell protection set in motion by MCF-7 cells were effective in counteracting the noxious stimulus exerted by this toxin under our experimental conditions.

The responses that we have detected when MCF-7 cells were exposed to both OA and GB consist of multiple patterns and show that the two agents that we have used in our study exert both independent and interacting actions in the same biological system. The patterns of interacting actions that we detected included synergism, similar effects that were maximally induced by each toxin alone and were not further enhanced by the combination of the two toxins, as well as antagonism. Our grouping represents a simplification, based on the general features of recorded effects for each component, under the three different experimental conditions that we have been used in this study, and we cannot exclude that patterns of cell responses to the combined toxins might be more complex. For instance, the antagonistic responses of set 2 might be grouped into two subsets. The first subset could comprise sets 2A and 2C and would include patterns consisting of components whose levels were undistinguishable from controls after combined treatment but were found to be decreased after treatment with one toxin and increased by the other one (Figure 6A,C and Figure S4 of the Supporting Information). The second subset, in turn, comprising sets 2B and 2D, would include components affected by only one toxin, whose levels would be rescued to control values by the combined presence of the other toxin (Figure 6B,D and Figure S4 of the Supporting Information). A better understanding of these patterns, however, demands a more thorough characterization of the kinetics and dose−effect relationships of those responses.

The limited information available about molecular responses of MCF-7 cells to the combined exposure of OA and GB constrains our discussion to some of the effects that we detected and classified among set 1, comprising the components whose levels were found to be affected by the combined treatment, regardless of the response recorded after the addition of only one agent. Within this frame, the results that we obtained about hsp27 appear mechanistically informative. In particular, the effects on phosphorylated and nonphosphorylated proteins can

Table 2. Classification of MCF-7 Cell Components Affected by Treatment with OA and GB[a]

Primary Set	Secondary Set	Mixture vs Controls	Mixture vs OA	Mixture vs GB	ssp	Components identification
1	A	Y	Y	Y	7105	Phosphoglycerate mutase 1
					4109	Heat shock protein beta-1
					7307	Poly(rC)-binding protein 1
					8002	Superoxide dismutase [Mn], mitochondrial [Precursor]
	B	Y	Y	N	5409	Myosin-7
	C	Y	N	Y	2109	Heat shock protein beta-1
					4101	Heat shock protein beta-1
					3106	Heat shock protein beta-1
	D	Y	N	N	3006	ATP synthase subunit d
					6106	Peroxiredoxin-6
					8003	Peroxiredoxin-5, mitochondrial [Precursor]
					2106	Catechol O-methyltransferase
					2008	Lactoylglutathione lyase
					5006	Nucleoside diphosphate kinase A
2	A	N	Y	Y	5010	Heat shock protein beta-1
					5113	Heat shock protein beta-1
					3010	Heat shock protein beta-1
	B	N	Y	N	5003	Superoxide dismutase [Cu-Zn]
					6004	Mesoderm development candidate 2
					6101	Protein-L-isoaspartate(D-aspartate) O-methyltransferase
					6105	Heat shock protein beta-1
					7001	40S ribosomal protein S12
					8005	Cofilin-1
					8012	Peptidyl-prolyl cis-trans isomerase A
					8116	Calcyclin-binding protein
					8503	ATP synthase subunit alpha, mitochondrial [Precursor]
					8013	Destrin
					9101	Coiled-coil-helix-coiled-coil-helix domain-containing protein 3, mitochondrial [Precursor]
					9901	Probable ATP-dependent RNA helicase DDX17
	C	N	N	Y	5004	Semenogelin-1 [Precursor]
	D	N	N	N	202	Methylosome subunit pICln
					2005	Thioredoxin
					7305	Sialic acid synthase
					9301	Fructose-bisphosphate aldolase A
					7110	Fumarylacetoacetate hydrolase domain-containing protein 1

[a] The experimental conditions are those of Figures 1−3. The components have been distributed in the different sets and subsets on the basis of the calculated p values and by indicating either the significance of the detected change (yes, Y; $p < 0.05$) or the lack of significance of the detected change (no, N; $p > 0.05$).

be distinguished, because the changes in the phosphorylation state of the protein are post-translational and then depend on a pool of hsp27 already existing in MCF-7 cells. In turn, the effects found on nonphosphorylated forms of hsp27 can depend on both covalent modification and turnover of the protein. Thus, the stabilization of phosphorylated hsp27 induced by OA is post-translational and independent of GB (Table 2, set 1, secondary set C; Figure 5). A different condition exists with regard to nonphosphorylated hsp27, as MCF-7 cell exposures to the two toxins separately lead to opposite responses (Table 1). Although it remains to be established whether the GB-induced increase in the cellular levels of nonphosphorylated hsp27 protein depends on increased synthesis or decreased disposal, the finding that the combined treatment of MCF-7 cells with OA and GB results in decreased levels of intact, nonphosphorylated hsp27 (SSP 5113) implies that OA antagonizes the effect of GB (Table 2, set 2, secondary set A; Figure 6).

Taking into consideration the preliminary nature of this study, our interpretations regarding the mechanistic basis of the responses induced by OA and GB in combination, whenever the two toxins appear to share their molecular end points (Table 2, set 1, secondary sets A and D), essentially represent a working hypothesis. We will then focus our discussion on only one protein component from each secondary set, as a reference response, to outline our working hypothesis (Figure 7).

The nonphosphorylated fragment of hsp27 (SSP 4109) is the case component of detected synergistic effects (Table 2, set 1, secondary set A). On the basis of the responses induced by OA and GB separately, it seems likely that an increased level of SSP 4109 is part of MCF-7 cell disposal induced by OA (*16*), whereas the same end point might stem from a normal rate of protein disposal in cells where GB has induced an increased level of hsp27 protein. Thus, synergism might result from differences in the rates of distinct molecular processes (protein

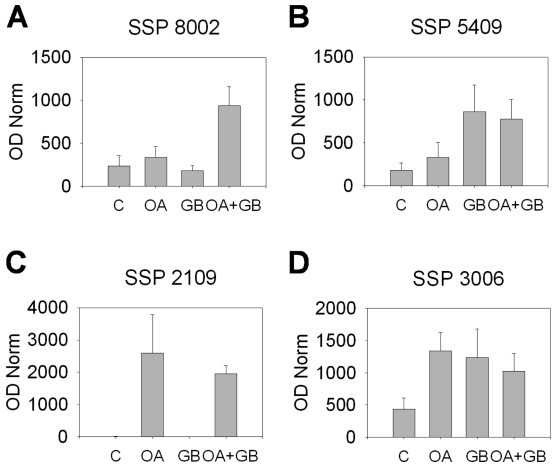

Figure 5. Patterns of responses in MCF-7 cells after a combined treatment with OA and GB. The patterns refer to the components whose levels were found to be significantly affected ($p < 0.05$) by the combined treatment (set 1). Cells were exposed to 50 nM OA, 50 nM GB, or the combined addition of the two toxins for 24 h, as indicated.

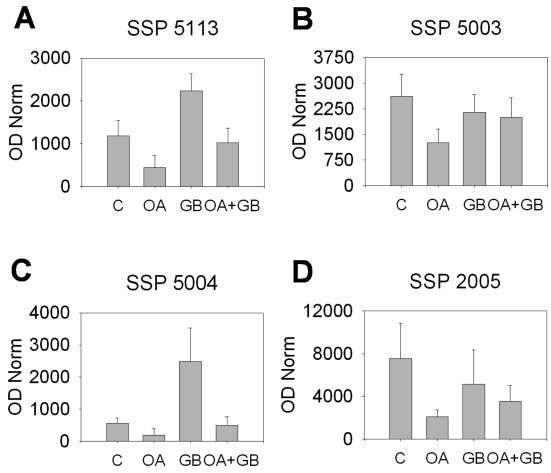

Figure 6. Patterns of responses in MCF-7 cells after a combined treatment with OA and GB. The patterns refer to the components that were found to be significantly affected ($p < 0.05$) in cells that had been challenged with only one toxin but not when cells had been subjected to the combined treatment (set 2). Cells were exposed to 50 nM OA, 50 nM GB, or the combined addition of the two toxins for 24 h, as indicated.

phosphorylation vs protein turnover) affected by the two toxins and eventually leading to the same end point.

A different situation might exist when combined effects of OA and GB do not significantly differ from those that they elicited when administered alone (Table 2, set 1, secondary set D). Focusing our attention on the increase in the cellular content of the ATP synthase subunit δ, the effect could take place through the same molecular machinery of a stress response, independently of the distinct events that originally triggered its activation in MCF-7 cells exposed to either OA (altered control of protein phosphorylation) or GB (impaired intracellular potassium homeostasis).

If the two mechanisms are matched, they could fit a unified model, where the two alternatives can be distinguished according to the location of the rate-limiting step in the toxicity pathways, which would occur either before (secondary set A) or after (secondary set D) the convergence of distinct sequences of molecular events triggered by the two toxins (Figure 7).

This mechanistic interpretation of our findings and our model is speculative, and further studies are needed to fully probe them, with specific reference to the kinetics and dose−effect relationships of response, as well as a deeper insight into other proteins that are expected to be mechanistically linked in the toxicity pathways triggered by the two toxins. In any case, the finding that the system, as such, responds to the combined challenge by multiple patterns indicates that cross-talks among the toxicity pathways of the two agents should be taking place at several levels, resulting in effects that are component-related (*5*). Indeed, extensive cross-talks among signal transduction pathways have already been reported, giving rise to multiple patters of response when simple systems are challenged by agents possessing distinct mechanisms of action (*36*). Taken as a whole, our system level analysis of molecular components in a cellular model shows that the combination of two biologically active agents possessing distinct molecular mechanisms of action triggers multiple patterns of responses in a simplified system, such as a cultured cell line.

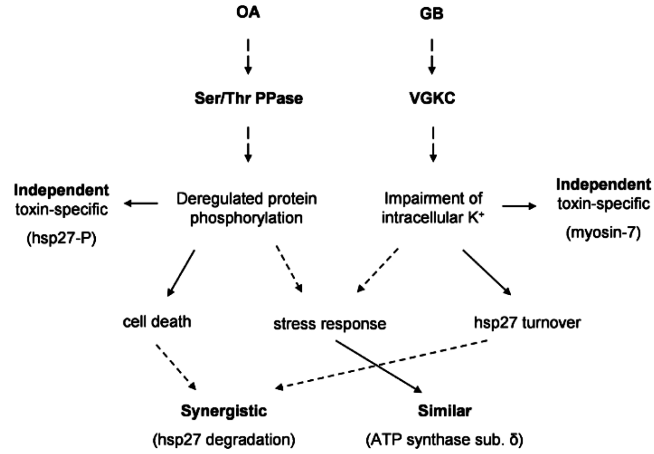

Figure 7. General model of the mechanisms responsible for synergism, independent, and similar actions exerted by a mixture of toxins acting through distinct molecular mechanisms of action. The model is based on the effects observed in MCF-7 cells that had been exposed to OA, GB, and the combination of the two toxins, and the arrows represent the steps of the mechanisms by which individual toxins build up their own responses. The solid lines indicate the portion of the toxicity pathways that includes the rate-limiting step in the process leading to individual responses. See the text for explanations.

Acknowledgment. We thank Adriano Benedetti and the Centro Interdipartimentale Grandi Strumenti at Università di Modena e Reggio Emilia for their skillful technical assistance in our MS analyses. This investigation was supported by the Italian MUR (Grant 2007FXSCL2).

Supporting Information Available: Additional information regarding the protein components affected by OA and GB in MCF-7 cells, including their classification based on functional annotation, data sets used for analysis of responses, the protein profiles obtained in our experiments, and the quantitative representation of the pattern of responses for the protein components not reported in Figures 5 and 6. This material is available free of charge via the Internet at http://pubs.acs.org.

References

(1) Ulrich, R., and Friend, S. H. (2001) Toxicogenomics and drug discovery: Will new technologies help us produce better drugs? *Nat. Rev. Drug Discovery 1*, 84–88.
(2) Benninghoff, A. D. (2007) Toxicoproteomics−The next step in the evolution of environmental biomarkers? *Toxicol. Sci. 95*, 1–4.
(3) Hamadeh, H. K., Bushel, P. R., Jaydev, S., DiSorbo, O., Bennett, L., Li, L., Tennant, R., Stoll, R., Barrett, J. C., Paules, R. S., Blanchard, K., and Afshari, C. A. (2002) Prediction of compound signature using high density gene expression profiling. *Toxicol. Sci. 67*, 232–240.

(4) Silva, E., Rajapakse, N., and Kortenkamp, A. (2002) Something from "nothing"—Eight weak estrogenic chemicals combined at concentrations below NOECs produce significant mixture effects. *Environ. Sci. Technol. 36*, 1751–1756.
(5) Rossini, G. P. (2005) Functional assays in marine biotoxin detection. *Toxicology 208*, 451–462.
(6) Hallegraeff, G. M. (2004) Harmful algal blooms: A global overview. In *Manual on Harmful Marine Microalgae*, 2nd ed. (Hallegraeff, G. M., Anderson, D. M., and Cembella, A. D., Eds.) pp 25−49, UNESCO, Paris.
(7) Jensen, G. L., and Greenlees, K. J. (1997) Public health issues in aquaculture. *Rev. Sci. Technol. 16*, 641–651.
(8) Roeder, R. A., Garber, M. J., and Schelling, G. T. (1998) Assessment of dioxins in foods from animal origins. *J. Anim. Sci. 76*, 142–151.
(9) Marcotrignano, G. O., and Storelli, M. M. (2003) Heavy metal, polychlorinated biphenyl and organochlorine pesticide residues in marine organisms: Risk evaluation for consumers. *Vet. Res. Commun. 27*, 183–195.
(10) Yasumoto, T., Murata, M., Oshima, Y., Sano, M., Matsumoto, G. K., and Clardy, J. (1985) Diarrhetic shellfish toxins. *Tetrahedron 41*, 1019–1025.
(11) Goto, H., Igarashi, T., Yamamoto, M., Yasuda, M., Sekiguchi, R., Watai, M., Tanno, K., and Yasumoto, T. (2001) Quantitative determination of marine toxins associated with diarrhetic shellfish poisoning by liquid chromatography coupled with mass spectrometry. *J. Chromatogr. A 907*, 181–189.
(12) MacKenzie, L., Holland, P., McNabb, P., Beuzenberg, V., Selwood, A., and Suzuki, T. (2002) Complex toxin profiles in phytoplankton and Greenshell mussels (*Perna canaliculus*), revealed by LC-MS/MS analysis. *Toxicon 40*, 1321–1330.
(13) Bialojan, C., and Takai, A. (1988) Inhibitory effect of a marine sponge toxin, okadaic acid, on protein phosphatases. *Biochem. J. 256*, 283–290.
(14) Ghiaroni, V., Sasaki, M., Fuwa, H., Rossini, G. P., Scalera, G., Yasumoto, T., Pietra, P., and Bigiani, A. (2005) Inhibition of voltage-gated potassium currents by gambierol in mouse taste cells. *Toxicol. Sci. 85*, 657–665.
(15) Fuwa, H., Kainuma, N., Tachibana, K., and Sasaki, M. (2002) Total synthesis of (−)-gambierol. *J. Am. Chem. Soc. 124*, 14983–14992.
(16) Malaguti, C., and Rossini, G. P. (2002) Recovery of cellular E-cadherin precedes replenishment of estrogen receptor and estrogen-dependent proliferation of breast cancer cells rescued from a death stimulus. *J. Cell. Physiol. 192*, 171–181.
(17) Bradford, M. (1976) A rapid and sensitive method for the quantitation of microgram quantities of protein utilizing the principle of protein-dye binding. *Anal. Biochem. 72*, 248–254.
(18) Bjellqvist, B., Ek, K., Righetti, P. G., Gianazza, E., Görg, A., Westermeier, R., and Postel, W. (1982) Isoelectric focusing in immobilized pH gradients: Principle, methodology and some applications. *J. Biochem. Biophys. Methods 6*, 317–339.
(19) Rabilloud, T. (1992) A comparison between low background silver diammine and silver nitrate protein stains. *Electrophoresis 13*, 429–439.
(20) Speicher, K. D., Kolbas, O., Harper, S., and Speicher, D. W. (2000) Systematic analysis of peptide recoveries from in-gel digestions for protein identifications in proteome studies. *J. Biomol. Technol. 11*, 74–86.
(21) Hosokawa, M., Tsukada, H., Saitou, T., Kodama, M., Onomura, M., Nakamura, H., Fukuda, K., and Seino, Y. (1998) Effects of okadaic acid on rat colon. *Dig. Dis. Sci. 43*, 2526–2535.
(22) Liu, J., and Sidell, N. (2005) Anti-estrogenic effects of conjugated linoleic acid through modulation of estrogen receptor phosphorylation. *Breast Cancer Res. Treat. 94*, 161–169.
(23) Miglietta, A., Bozzo, F., Gabriel, L., Bocca, C., and Canuto, R. A. (2006) Extracellular signal-regulated kinase 1/2 and protein phosphatase 2A are involved in the antiproliferative activity of conjugated linoleic acid in MCF-7 cells. *Br. J. Nutr. 96*, 22–27.
(24) Ouadid-Ahidouch, H., and Ahidouch, A. (2008) K^+ channel expression in human breast cancer cells: involvement in cell cycle regulation and carcinogenesis. *J. Membr. Biol. 221*, 1–6.
(25) Goldberg, A. L., and St. John, A. C. (1976) Intracellular protein degradation in mammalian cells: Part 2. *Annu. Rev. Biochem. 45*, 747–803.
(26) Kiguchi, K., Glesne, D., Chubb, C. H., Fujiki, H., and Hubermann, E. (1994) Differential induction of apoptosis in human breast tumor cells by okadaic acid and related inhibitors of protein phosphatases 1 and 2A. *Cell Growth Differ. 5*, 995–1004.
(27) Rossini, G. P. (2000) Neoplastic activity of DSP toxins: The effects of okadaic acid and related compounds on cell proliferation: Tumor promotion or induction of apoptosis? In *Seafood and Freshwater Toxins* (Botana, L. M., Ed.) pp 257−288, Marcel Dekker, New York.
(28) De Lamirande, E., Yoshida, K., Yoshiike, T. M., Iwamoto, T., and Gagnon, C. (2001) Semenogelin, the main protein of semen coagulum, inhibits human sperm capacitation by interfering with the superoxide anion generated during the process. *J. Androl. 22*, 672–679.
(29) Lanneau, D., Brunet, M., Frisan, E., Solary, E., Fontenay, M., and Garrido, C. (2008) Heat shock proteins: Essential proteins for apoptosis regulation. *J. Cell. Mol. Med. 12*, 743–761.
(30) Garrido, C. (2002) Size matters: of the small HSP27 and its large oligomers. *Cell Death Differ. 9*, 483–485.
(31) Kato, K., Hasegawa, K., Goto, S., and Inaguma, Y. (1994) Dissociation as a result of phosphorylation of an aggregated form of the small stress protein, hsp27. *J. Biol. Chem. 269*, 11274–11278.
(32) Rogalla, T., Ehrnsperger, M., Preville, X., Kotlyarov, A., Lutsch, G., Ducasse, C., Paul, C., Wieske, M., Arrigo, A.-P., Buchner, J., and Gaestel, M. (1999) Regulation of hsp27 oligomerization, chaperone function, and protective activity against oxidative stress/Tumor Necrosis Factor α by phosphorylation. *J. Biol. Chem. 274*, 18947–18956.
(33) Ferrero-Gutiérrez, A., Pérez-Gómez, A., Novelli, A., and Fernández-Sánchez, M. T. (2008) Inhibition of protein phosphatases impairs the ability of astrocytes to detoxify hydrogen peroxide. *Free Radical Biol. Med. 44*, 1806–1816.
(34) Yu, J. H., Yun, S. Y., Lim, J. W., Kim, H., and Kim, K. H. (2003) Proteome analysis of rat pancreatic acinar cells: Implication for cerulein-induced acute pancreatitis. *Proteomics 3*, 2446–2453.
(35) Basso, M., Giraudo, S., Corpillo, D., Bergamasco, B., Lopiano, L., and Fasano, M. (2004) Proteome analysis of human substantia nigra in Parkinson's disease. *Proteomics 4*, 3943–3952.
(36) Natarajan, M., Lin, K.-M., Hsueh, R. C., Sternweis, P. C., and Ranganathan, R. (2006) A global analysis of cross-talk in a mammalian cellular signalling network. *Nat. Cell Biol. 8*, 571–580.

TX900044P